Photochemistry and Photobiology, 2018, 94: 829–833

Photochemistry and Photophysics of Shinorine Dimethyl Ester†

Dalila E. Orallo[1], María Florencia Fangio[1], Martin Poblet[2], Mario O. Carignan[3], Luis Bernal[2], José I. Carreto[3], Sonia G. Bertolotti[4] and María Sandra Churio[1]*

[1]Departamento de Química, Facultad de Ciencias Exactas y Naturales, Instituto de Investigaciones Físicas de Mar del Plata (CONICET-UNMDP), Universidad Nacional de Mar del Plata, Mar del Plata, Argentina
[2]Departamento de Física, Facultad de Ciencias Exactas y Naturales, Universidad Nacional de Mar del Plata, Mar del Plata, Argentina
[3]Instituto Nacional de Investigación y Desarrollo Pesquero, Mar del Plata, Argentina
[4]Departamento de Química, Universidad Nacional de Río Cuarto, CONICET, Río Cuarto, Argentina

Received 7 November 2017, accepted 5 December 2017, DOI: 10.1111/php.12884

ABSTRACT

The photostability and photophysical properties of the dimethyl ester of the mycosporine-like amino acid shinorine have been experimentally evaluated in aqueous solution and in the presence of direct micelles prepared with a cationic or an anionic detergent, respectively. In comparison with shinorine, the ester molecule increases the photostability, the fluorescence quantum yield and the fluorescence lifetime in water as well as in the micellar solutions. The effects are more pronounced in sodium dodecyl sulfate solutions and suggest that the electrostatic attractions with the micellar interface contribute to limit the movement of the molecules and influence the relative rate of their deactivation channels. However, the predominance of the nonradiative decay is maintained together with the UV photoprotective ability of this atypical mycosporine species.

INTRODUCTION

The ubiquitousness, strong absorption in the ultraviolet (UV) and high photostability of natural mycosporine-like amino acids (MAAs) have attracted the attention of experts from photobiology to evolution fields (1,2). The UV radiation produces a broad spectrum of genetic and cytotoxic effects in aquatic organisms. At the beginning of the evolution of life on Earth, UVB flux rates clearly exceeded the present values, thus several protection strategies such as avoidance, screening, photochemical quenching and repair have evolved to counteract the negative effects of UV radiation (3). Experimental evidence indicates that in marine and freshwater organisms, the major functions of MAAs are to act as photoprotective UV filters and/or to work as antioxidants (4). The unique properties of MAAs have also motivated to explore their incorporation to nanocomposites as photocatalysts or UV sensors (5,6), and to ZnO nanoparticles and biopolymers as innovative green materials (7,8). Above all, however, MAAs have been proposed as active ingredients in the formulation of suncare lotions within the efforts to achieve more efficient alternatives for UV protection upon the worldwide increasing incidence of melanoma (9–11). Moreover, the rational design of new synthetic photoprotective compounds inspired in MAAs molecular structures has been recently reported (12). Interestingly, the substitution scheme of the characteristic structural core of mycosporines (oxo-mycosporines) and MAAs allow fine-tuning of their UV absorption maxima, although it is not clear in which extent their chemical and photochemical behavior may be affected too (13).

Some atypical forms of MAAs, such as methyl esters of shinorine, have been found in dinoflagellates and other marine species (4,14,15). The structure of one of these forms, named after M-333, has been confirmed by HPLC-MS and comparison with synthetic derivatives and NMR spectra (16). As MAAs are very soluble in water, this and other less polar derivatives of MAAs appear as promissory choices for the formulation of UV sunscreens. While their basic chemistry has been less considered, it is important to know, particularly in the field of sunscreens elaboration, the underlying photochemistry and performance in different matrixes, for example, creams and emulsions for topical applications.

With this approach, we have recently reported on the photophysicochemical characterization of the MAAs shinorine and porphyra-334 in the presence of direct ionic micelles. The study suggests that electrostatic interactions with the organized microheterogeneous environments may alter the reorientation molecular movements of the MAAs and influence the competition between their relaxation pathways. In fact, the enhancement of the fluorescence quantum yields and lifetimes of both MAAs in cetyltrimethylammonium chloride (CTAC) micellar systems seems to arise from the electrostatic attractions between the carboxylate group of the amino acid moieties and the cationic heads of the surfactant (18).

The esterification of the carboxylic functional groups provides a way to modify the polarity of the MAAs and, at the same time, it allows blocking their zwitterionic character under neutral pH (see Fig. 1). This in turn offers a strategy to explore the effect of structural variations, and discern the relevant interactions with charged microenvironments which can be found both in natural or artificial systems.

This work aims to evaluate comparatively the UV photoprotective ability and photophysical properties of one form of derivatized shinorine shown in Fig. 1, the shinorine dimethyl ester (SDME), in aqueous solution and in the presence of direct

*Corresponding author email: schurio@mdp.edu.ar (M. S. Churio)
†This article is part of a Special Issue commemorating the XIII ELAFOT Conference (23–27 October 2017 - Villa Carlos Paz, Cordoba, Argentina).

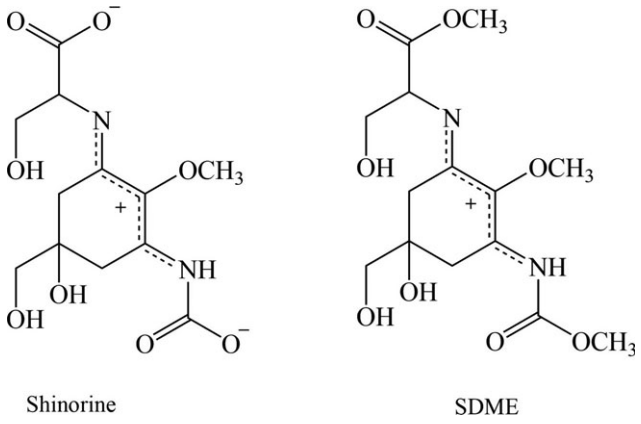

Figure 1. Molecular structures of shinorine and shinorine dimethyl ester (SDME).

micelles prepared with CTAC and with sodium dodecyl sulfate (SDS), that is, a cationic and an anionic detergent, respectively.

MATERIALS AND METHODS

Obtention of shinorine and its dimethylester. The MAA shinorine was extracted from the red alga *Porphyra leucosticta* and isolated according to the procedure reported previously (18). The aqueous solution of purified shinorine was dehydrated by lyophilization and treated, according to the Fischer esterification method, with BF_3-methanol complex for synthesis (20% in methanol, Merck) in sealed tubes during 40 min at 60°C (19, 20). To obtain the diester derivative, the molar fraction of alcohol relative to shinorine in the initial reaction mixture was larger than the stoichiometric ratio.

The presence of the reaction product in the final mixture was verified spectrophotometrically by the shift of the absorption maximum from 334 nm (shinorine) to 330 nm (SDME) (16,18). The SDME was finally separated from underivatized shinorine through isocratic HPLC (Konik KNK-500-A) with 0.05% v/v acetic acid as the mobile phase and a Lichrocart® TC-C18 column (5 μm, 4 mm ID × 25 cm), at room temperature and absorbance detection at 334 nm. Under these conditions, the retention time was 13.1 min for shinorine and 24.1 min for SDME. The identity of the derivatized product was confirmed by gradient HPLC (Shimadzu LC 10 A) by comparison with standard samples of esterified shinorine from natural origin, according to the report from Carignan and Carreto (16). In this case, a binary eluent gradient was used as follows: A (0.2% v/v formic acid and ammonium hydroxide, pH 3.05) and B (0.2% v/v formic acid and ammonium hydroxide, pH 3.05: methanol: acetonitrile, 80:10:10 in volume); together with two C18 columns in series (double endcapped Alltima, Alltech 5 μm, 4.6 × 150 mm, and CapCell Pack UG, Shiseido, Tokyo, Japan, 5 μm, 4.6 × 250 mm) at 40°C and detection at 330 nm. For this analysis, the retention time of SDME yielded 25 min. The SDME solutions were stored at −20°C till used.

Preparation of the micellar solutions. SDS was Sigma-Aldrich (>99%). CTAC (Sigma-Aldrich, 25% solution) was previously purified by evaporation to dryness and recrystallization from a 50% ethanol–acetone mixture. Solutions were prepared by dissolving 0.10 mol L^{-1} of the solid surfactant in tridistilled water (this concentration is greater than the corresponding critical micellar concentration). An aliquot of concentrated SDME in the same solvent was added into the micellar solution.

UV-vis absorption and photostability studies. Absorption spectra of the solutions were determined in 1-cm path length quartz cells with a double beam UV-visible spectrophotometer (Shimadzu UV-PC 2101). The concentrations were between 2.2×10^{-6} mol L^{-1} and 4.5×10^{-6} mol L^{-1}.

Photodegradation quantum yields were evaluated by irradiation of the solutions in the same quartz cells with a suntanning lamp (Philips CLEO UV- HPA 400S) and a pass filter allowing wavelengths larger than 320 nm. The time evolution of the SDME concentration was monitored by UV absorption analysis. All the experiments were carried out by triplicate, at room temperature and with continuous stirring of the sample solution. An aqueous solution of shinorine with matched absorbance at maximal wavelength was used as the actinometer reference for the quantum yield calculations. The photodecomposition rate was obtained from the slope of the linear plot of the absorbance at 330 nm *vs* irradiation time.

Emission properties. Fluorescence spectra were acquired in 1-cm quartz cells by means of a Fluorolog-3 (FL3, Horiba Jobin Yvon) spectrofluorometer, equipped with nanoLEDs as the excitation light sources, an iHR320 grating monochromator and a TBX-04 photomultiplier connected to a TBX-PS power supply. The FluoroHub-B photon counting module was controlled by a DataStation for the data acquisition. Water and micellar solutions of 2.3×10^{-6} mol L^{-1} SDME were excited at 340 nm for the emission spectra, and the emission was observed at 420 nm for the excitation spectra.

The fluorescence quantum yields Φ_f were determined from the area under the emission spectrum curves for SDME and shinorine solutions with matched absorbances, as described by Orallo *et al.* (18). Shinorine in water ($\Phi_f = 1.6 \times 10^{-4}$) was taken as the standard for the quantum yield calculations (21). Fluorescence lifetimes were measured on the same solutions by time-correlated single photon counting (TCSPC) with a FL3 TCSPC-SP (Horiba Jovin Yvon) instrument. Biexponential functions were appropriate for fitting the decays, yielding residues within the ±4 interval. The contribution amounting *ca.* 95% of the signal was identified as the fluorescence lifetime τ_f.

Laser-induced optoacoustic determinations. The instrumental setup consisted of a pulsed N_2 laser (337 nm, 100 μJ- and 1 ns-pulses) built at the UNMDP, and a piezoelectric detector (PZT, 2.5 MHz) with the amplifier and the power supply from CiOP-UNLP (Argentina) connected to two oscilloscopes of 100 MHz in a Faraday cage for data acquisition. The sample solutions were placed in a spectrophotometric quartz cuvette in a thermostated holder. The laser beam entered the sample and made focus in its center by means of a cylindrical lens. The focus zone was rectangular and had a width <1 mm at a right angle configuration relative to the optoacoustic detector. A neutral density filter allowed for variations in the intensity of the incident laser pulses. Potassium dichromate (Mallinckrodt p.a.) was used as the calorimetric reference. All the solutions were prepared by matching the absorbance in 0.18 at 337 nm. The amplitude of the signals H was determined as the peak to peak distance between the first maximum and the first minimum of the acoustic wave. Linear dependence of H with laser energy fluence E_0 was verified. Energy normalized signals, H_n, were obtained as the slopes of the linear plots of H *vs* E_0 (21,22).

RESULTS AND DISCUSSION

The absorption spectra of SDME in different media are shown in Fig. 2. For comparison purposes, the wavelengths of maximal absorption (λ_{max}), together with previously reported values for shinorine in the same media (18), are summarized in Table 1. The SDME bands move toward shorter wavelengths with respect to the absorption of shinorine in water (λ_{max} = 334 nm). Besides, the peaks for SDME in micellar solutions exhibit slight redshifts from the position in aqueous solution.

The emission spectra (Fig. 3) show other noticeable effects. The displacements and intensity changes of the fluorescence bands are generally larger, and they depend on the type of surfactant. Excitation spectra in the different media (not shown) are coincident with the respective absorption profiles, confirming the emissions to be originated from the first singlet excited state of SDME.

The fluorescence parameters compiled in Table 1 indicate that the dimethyl ester exhibits emission at larger energies than shinorine. The shift is more pronounced in SDS (16 nm). In addition, the intensity of the fluorescence of SDME is clearly enhanced in the presence of SDS micelles, whereas in water and CTAC, they are similar. This is consistently evidenced in the results of Φ_f, the fluorescence quantum yields (see Table 1), which increase between three and four times in SDS, and in a

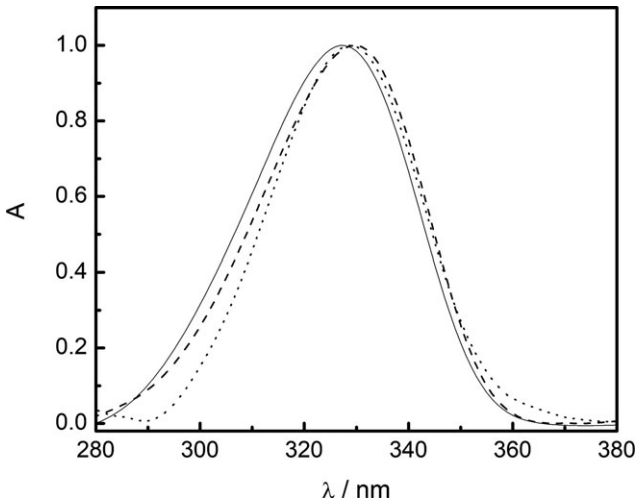

Figure 2. Normalized UV absorption spectra of shinorine dimethyl ester (SDME) in H_2O (——), 0.1 mol L^{-1} SDS (- - -), and 0.1 mol L^{-1} CTAC (···).

Table 1. Photochemical and photophysical properties of shinorine and its dimethyl ester in different media.

	Shinorine dimethyl ester			Shinorine*		
Medium	H_2O	SDS	CTAC	H_2O	SDS	CTAC
λ_{abs}/nm	328.0	330.0	329.0	334.0	334.0	334.5
λ_{em}/nm	414.0	408.0	416.0	424.0	424.0	418.0
$\Delta\bar{\nu}$/cm^{-1}	6333	5793	6356	6355	6266	5971
$\Phi_f/10^{-4}$	13.4	40.0	9.8	1.6	1.6	3.3
τ_f/ns	13.6	21.2	11.6	0.58	0.75	0.87
$\Phi_d/10^{-4}$	1.0	0.5	n.d.†	3.4	3.1	1.2

*Values previously reported by Orallo *et al.* (ref. 18). †Not determined.

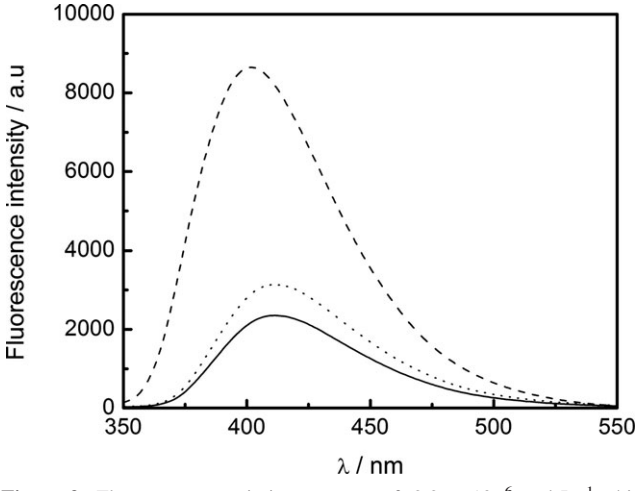

Figure 3. Fluorescence emission spectra of 2.3×10^{-6} mol L^{-1} shinorine dimethyl ester (SDME) in H_2O (——), 0.1 mol L^{-1} SDS (- - -), and 0.1 mol L^{-1} CTAC (···).

ratio of 3 to 25 in comparison with shinorine in the same environment. The enhancements of the emission correlate with the decrease in the values of Stokes shifts, $\Delta\bar{\nu}$ (see Table 1). In fact, they amount almost the same in water and in CTAC, but it diminishes in SDS where Φ_f is maximal.

All these effects suggest that the presence of anionic SDS micelles limits the movement of SDME molecules. This can be explained by electrostatic attractions between the positive charges on SDME and the micellar interface.

Electrostatic interactions have been already invoked to account for the micellar effects in the photophysics of the MAAs shinorine and porphyra-334 in SDS and CTAC solutions (18). The results of that previous study support the preferential solubilization of the MAAs in the aqueous phase outside the direct micelles and, due to the zwitterionic character of the natural compounds under physiologic pH, the possibility of columbic interactions with the charged heads of the surfactants. However, in that case, the most marked effects were observed in the presence of CTAC, instead of SDS micelles, pointing to the dominance of attractions between the anionic carboxylate groups in the MAA and the cationic heads of CTAC. Recalling that the derivatization of shinorine yielding SDME converts the carboxylic groups into methyl ester groups, the negative charges from carboxylates are avoided and only the positive charges on protonated nitrogen atoms remain (Fig. 1). Thus, the relevant electrostatic attractions are expected to arise with SDS, that is, in the presence of anionic micelles, and not with CTAC, in full agreement with our present results.

As expected, according to this interpretation, the results from TCSPC on the fluorescence lifetimes of SDME (Table 1) are similar for aqueous and CTAC solutions but increase around two-fold in SDS. Besides, all the τ_f values are one order of magnitude larger than for shinorine in the same medium.

On the other hand, the slopes of the linear plots of the absorbance evolution during the photolysis experiments (Fig. 4) indicate that SDME improves the photostability with respect to shinorine. Indeed, the parameters in Table 1 account for relative decreases in the photodecomposition quantum yields by factors of two in water and of six in SDS solution. Thus, the effects in micellar media for SDME are in line with the results for shinorine and porphyra-334: the stronger coulombic attractions with the micellar surface, the better protection toward photodecomposition (18).

Finally, these interactions seem to promote the radiative deactivation of the excited states, although the competition between

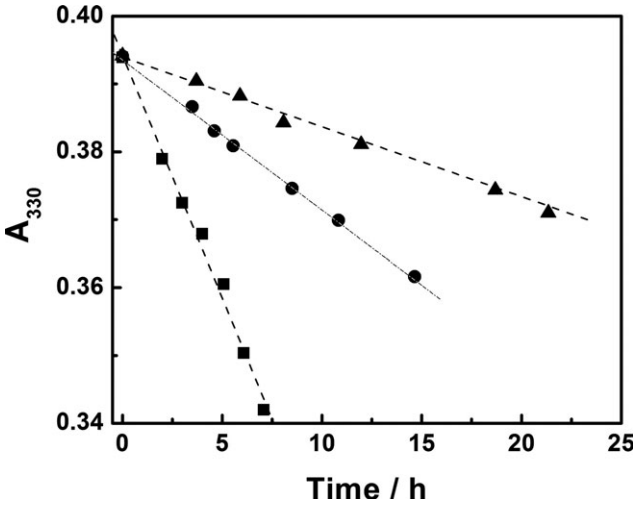

Figure 4. Plots of the absorbance at 330 nm *vs* irradiation time: shinorine dimethyl ester (SDME) in H_2O (-●-), SDME in 0.1 mol L^{-1} SDS (-▲-), and shinorine in H_2O (-■-).

radiative, reactive and nonradiative channels is still dominated by the last one. This is clear from the results of the laser-induced optoacoustic spectroscopy: The values of H_n for SDME and the calorimetric reference in SDS solution at 21°C are equal, within the experimental uncertainties. The same is observed at 6.5°C and for shinorine as well. These results evidence the almost exclusive thermal origin of the optoacoustic signals and confirm that both, SDME and shinorine, deliver most of the absorbed UV energy as heat, supporting the nonradiative decay as the main deactivation process.

Besides, the experiments agree with the chemical calculations in conceiving the thermal deactivation of photon activated MAAS as a very efficient and rapid process that takes place *via* conical intersections of the potential energy surfaces (21–23). It seems reasonable to assume, for shinorine and SDME, the same mechanism that explains the transition from S_1 to S_0 electronic states of the MAA palythine, according to the computational studies carried out by Sampedro (23). This implies the out-of-plane movement of the imine group, the simultaneous approach of the adjacent carbon atoms while the rest of the alkene moiety remains almost planar. However, the structural variation ongoing from shinorine to SDME may influence enough the relative rate of the nonradiative deactivation pathway to enlarge the lifetime of the S_1 state and consequently increase both fluorescence parameters: τ_f and Φ_f.

It is interesting to point out that these findings may be relevant from the bioenergetic point of view as well. The role of MAAs as accessory pigments in photosynthesis was postulated in a very early report by Sivalingam *et al.* (24). The fluorescence emission of MAAs overlaps the Soret band of chlorophylls, so that the energy transfer could be theoretically possible. However, this idea was poorly supported by the low fluorescence yields observed in aqueous solutions (21,25,26). Recently, this notion has reemerged in a study of the symbiotic association between a novel dinoflagellate from Ross Sea, Antarctica and the microalga *Phaeocystis antarctica* (27). The evidences point to the occurrence of two populations of MAAs, one located in the cytoplasm and the other in the plastids. Specifically, the MAAs within the plastids may act as light-harvesting supplements in the photosynthetic organisms through the Förster resonance energy transfer (FRET) mechanism. As the efficiency of FRET depends strongly on the fluorescence yield of the donor and on the proximity to the acceptor, our observations are in line with the hypothetically significant contributions to the energy transfer within the organelle rather than in the more fluidic cytoplasm environment, even considering similar distances between the MAAs and chlorophylls (27).

CONCLUSIONS

Transformation of natural shinorine by methylation of the carboxylic groups enhances its photostability in aqueous solutions and in the presence of SDS micelles. The fluorescence lifetimes and quantum yields are also increased; the effect is much more pronounced in SDS solutions than in water or in CTAC solutions. Thus, it is evident that modifications in the substitution pattern of MAA structure and the characteristics of the media affect their photophysicochemical behavior. In particular, the speciation of the natural molecule and the interactions with charged micro-heterogeneous environments are relevant. The net positive charges on the SDME enable electrostatic attractions with the anionic heads of SDS on the micelle surface. This seems to alter the relative contribution of the deactivation channels of the excited state, probably due to a larger degree of hindrance in the molecular movements in the micelle/water interface. Still, the nonradiative decay is the major deactivation process, thus confirming the preservation of the UV photoprotective ability of the diester species and suggesting that less polar derivatives of MAAs are promising as UV filter ingredients in the suncare formulations.

Acknowledgements—This work was supported by UNMDP (EXA 759/16- 15/E710) and CONICET (PIP 2010-0284). SGB thanks to UNRC. The authors are also grateful to Dr. Carolina Lorente (INIFTA, Universidad Nacional de La Plata) for providing the fluorescence instrumental facilities and to Dr. Federico R. Conde (UNMDP) for his help in the derivatization procedure.

REFERENCES

1. Gao, Q. and F. Garcia-Pichel (2011) Microbial ultraviolet sunscreens. *Nat. Rev. Microbiol.* **9**, 791–802.
2. Michaelian, K. and A. Simeonov (2015) Fundamental molecules of life are pigments which arose and co-evolved as a response to the thermodynamic imperative of dissipating the prevailing solar spectrum. *Biogeosciences* **12**, 4913–4937.
3. Roy, S. (2000) Strategies for the minimization of UV-induced damage. In *The effects of UV radiation in the marine environment* (Edited by S. de Mora, S. Demers and M. Vernet), pp. 177–205. Cambridge University Press, Cambridge, UK.
4. Carreto, J. I. and M. O. Carignan (2011) Mycosporine–like amino acids: Relevant secondary metabolites. Chemical and ecological aspects. *Mar. Drugs* **9**, 387–446.
5. Kim, H. U., S. Ha, D. Amalnerkar, S. Y. Kim, C. Ahn, Y. T. Lim, M. H. Lee, B. J. Moon, S. Bae, S. H. Moh, A. Kulkarni and T. Kim (2017) MoS2-graphene-mycosporine-like amino acid nanocomposite as photocatalyst. *NANO* **12**, 1750019.
6. Jin, Y., A. Kulkarni, H. Qin, D. H. Kim, Y. W. Yu, J. C. Lee, T. Kim and S. H. Moh (2014) In-situ synthesis of polypyrrole-mycosporine like amino acid nanocomposite film for resistive UV-B sensor. *Sens. Lett.* **12**, 1736–1740.
7. Singh, G., P. K. Babele, A. Srivastava, R. P. Sinha and M. B. Tyagi (2014) Synthesis of ZnO nanoparticles using the cell extract of the cyanobacterium, Anabaena strain L31 and its conjugation with UV-B absorbing compound shinorine. *J. Photochem. Photobiol., B* **138**, 55–62.
8. Fernandes, S. C. M., A. Alonso-Varona, T. Palomares, V. Zubillaga, J. Labidi and V. Bulone (2015) Exploiting mycosporines as natural molecular sunscreens for the fabrication of UV-absorbing green materials. *Appl. Mater. Interfaces* **7**, 16558–16564.
9. Morabito, K., N. C. Shapley, K. G. Steeley and A. Tripathi (2011) Review of sunscreen and the emergence of non-conventional absorbers and their applications in ultraviolet protection. *Int. J. Cosmet. Sci.* **33**, 385–390.
10. Colabella, F., M. Moliné and D. Libkind (2014) UV Sunscreens of microbial origin: Mycosporines and mycosporine-like aminoacids. *Recent Pat. Biotechnol.* **8**, 179–193.
11. WHO World Health Organization (2017) Ultraviolet radiation. Skin cancers. How common is skin cancer? Available at: http://www.who.int/uv/faq/skincancer/en/index1.html. Accessed on 20 October 2017.
12. Losantos, R., I. Funes-Ardoiz, J. Aguilera, E. Herrera-Ceballos, C. García-Iriepa, P. J. Campos and D. Sampedro (2017) Rational design and synthesis of efficient sunscreens to boost the solar protection factor. *Angew. Chem. Int. Ed. Engl.* **56**, 2632–2635.
13. Oda, Y., Q. Zhang, S. Matsunaga, M. J. Fujita and R. Sakai (2017) Two new mycosporine-like amino acids LC-343 and mycosporine-ethanolamine from the micronesian marine sponge *Lendenfeldia chondrodes*. *Chem. Lett.* **46**, 1272–1274.
14. Carreto, J. I., M. O. Carignan and N. G. Montoya (2001) Comparative studies on mycosporine-like amino acids, paralytic shellfish toxins and pigment profiles of the toxic dinoflagellates *Alexandrium tamarense*, *A. catenella* and *A. minutum*. *Mar. Ecol. Prog. Ser.* **223**, 49–60.

15. Laurion, I. and S. Roy (2009) Growth and photoprotection in three dinoflagellates (including two strains of Alexandrium tamarense) and one diatom exposed to four weeks of natural and enhanced UVB radiation. *J. Phycol.* **45**, 16–33.
16. Carignan, M. O. and J. I. Carreto (2013) Characterization of mycosporine-serine-glycine methyl ester, a major mycosporine-like amino acid from dinoflagellates: A mass spectrometry study. *J. Phycol.* **49**, 680–688.
17. Losantos, R., D. Sampedro and M. S. Churio (2015) Photochemistry and photophysics of mycosporine-like amino acids and gadusols, nature's ultraviolet screens. *Pure Appl. Chem.* **87**, 979–996.
18. Orallo, D. E., S. G. Bertolotti and M. S. Churio (2017) Photophysicochemical characterization of mycosporine-like amino acids in micellar solutions. *Photochem. Photobiol. Sci.* **16**, 1117–1125.
19. Lamavreux, G. and C. Agüero (2009) A comparison of several modern alkylating agents. *ARKIVOC*, **I**, 251–264.
20. Otero, J. and J. Nishikido (2010) *Esterification. Methods, reactions, and applications*. 2nd Ed. Wiley-VCH, Hoboken, NJ.
21. Conde, F. R., M. S. Churio and C. M. Previtali (2004) The deactivation pathways of the excited-states of the mycosporine-like amino acids shinorine and porphyra- 334 in aqueous solution. *Photochem. Photobiol. Sci.* **3**, 960–967.
22. Conde, F. R., M. S. Churio and C. M. Previtali (2007) Experimental study of the excited state properties and photostability of the mycosporine-like amino acid palythine in aqueous solution. *Photochem. Photobiol. Sci.* **6**, 669–674.
23. Sampedro, D. (2011) Computational exploration of natural sunscreens. *Phys. Chem. Chem. Phys.* **13**, 5584–5586.
24. Sivalingam, P. M., T. Ikawa and K. Nisizawa (1976) Physiological roles of a substance 334 in algae. *Bot. Mar.* **19**, 9–21.
25. Moisan, T. A. and B. G. Mitchell (2001) UV absorption by mycosporine-like amino acids in *Phaeocystis antarctica* Karsten induced by photosynthetically available radiation. *Mar. Biol.* **138**, 217–227.
26. Oren, A. and N. Gunde-Cimerman (2007) Mycosporines and mycosporine-like amino acids: UV protectants or multipurpose secondary metabolites?. *FEMS Microbiol. Lett.* **269**, 1–10.
27. Stamatakis, K., D. Vayenos, C. Kotakis, R. J. Gast and G. C. Papageorgiou (2017) The extraordinary longevity of kleptoplasts derived from the Ross Sea haptophyte *Phaeocystis antarctica* within dinoflagellate host cells relates to the diminished role of the oxygen-evolving Photosystem II and to supplementary light harvesting by mycosporine-like amino acid/s. *Biochim. Biophys. Acta* **1858**, 189–195.